Renewable and Sustainable Energy Reviews 24 (2013) 406–417

Contents lists available at SciVerse ScienceDirect

Renewable and Sustainable Energy Reviews

journal homepage: www.elsevier.com/locate/rser

Solar desalination based on multiple effect humidification process: Thermal performance and experimental validation

Khalifa Zhani *

Laboratoire des Systèmes Electro-Mècaniques (LASEM), National Engineering School of Sfax, Sfax University, Sfax, Tunisia

ARTICLE INFO

Article history:
Received 12 October 2012
Received in revised form
4 March 2013
Accepted 15 March 2013
Available online 22 April 2013

Keywords:
Solar energy
Water desalination
Steady state
Modeling
Experimental validation
GOR

Abstract: The present paper deals with a theoretical and experimental study of a new generation of water desalination unit by solar energy using the humidification and dehumidification (HD) principle is constructed at the national engineering school of Sfax (34N, 10E), Tunisia. The good quality of distilled water obtained by this new concept favours its use for producing water for drinking and irrigation. A mathematical model based on heat and mass transfers in each component of the unit is developed. The resulting ordinary differential systems of equations are transformed into a system of algebraic equations using the orthogonal collocation method (OCM) and simulated using C++ software in a steady state regime. The numerical model is used to investigate the thermal performance of this kind of installation exposed to a variation of the control parameters. The thermal performance was evaluated by the gained output ratio (GOR) and the efficiency of the water solar collector. A series of experiments was conducted and compared with the simulation results to validate the developed models. As a result, the proposed models can be used for sizing and testing the behaviour of such a type of desalination unit.

Contents

1. Introduction

In many places world wide drinkable water is already a scarce good and its lack will rise dramatically in the future. Missing energy sources and no grid connections complicates the use of standard desalination techniques in these places. Today, sea and brackish water desalination plants are well developed in industrial scales to provide big cities with fresh water. Small villages or settlements in rural remote areas without infrastructure do not profit from these techniques. The technical complexity of the large plants is very high and cannot easily be scaled down to very small systems and water demands. Furthermore, the lack of energy sources as well as a missing connection to the grid complicates the use of standard desalination techniques in these places. In arid and

* Tel.: +216 227 267 49.
E-mail address: zhani_khalifa@yahoo.fr

1364-0321/$ - see front matter © 2013 Elsevier Ltd. All rights reserved.
http://dx.doi.org/10.1016/j.rser.2013.03.064

Nomenclature

A	air–water exchanger area in the condensation tower (m^2)
a	air–water exchanger area in the evaporation tower (m^2)
C_e	water specific heat (J/kg/K)
C_w	water specific heat (J/kg/K)
C_g	moist air specific heat in the evaporation tower (J/kg/K)
C_G	moist air specific heat in the condensation tower (J/kg/K)
D_e	water mass velocity in the condensation tower ($kg/m^2/s$)
D_{h1}	hydraulic diameter of air flow (m)
D_{h2}	hydraulic diameter of water flow (m)
e	thickness of the condenser plate (m)
g	gravitational acceleration (m/s^2)
G	mass velocity of humid air ($kg/m^2/s$)
G_r	Grashof number
h_c	heat transfer coefficient for the condensate film ($W/m^2/K$)
h_g	air heat transfer coefficient at the air–water interface in evaporator ($W/m^2/K$)
h_e	heat transfer coefficient at the water-condenser inside wall interface ($W/m^2/K$)
h_l	water heat transfer coefficient at the air–water interface in evaporator ($W/m^2/K$)
h_G	air film heat transfer coefficient in the condensation tower ($W/m^2/K$)
l	width of water solar collector (m)
L	water mass flow rate in the evaporation tower ($kg/m^2/s$)
I	solar flux (W/m^2)
k	water vapor mass transfer coefficient at the air–water interface ($W/m^2/K$)
m_w	water flow rate in the water solar collector (kg/s)
m_c	fresh water production (kg/s)
Pr	Prandtl number
Re	Reynolds number
P_i	saturation pressure (Pa)
T	temperature (K)
T_i	temperature at the air–water interface in the evaporation tower (K)
T_{ic}	temperature at the air–water interface in the condensation tower (K)
T_p	wall temperature (K)
S	water solar collector area (m^2)
U	overall heat transfer coefficient in the condensation tower ($W/m^2/K$)
U_w	overall energy loss from the absorber to outside ($W/m^2/K$)
W	air humidity (kg water/kg dry air)
W_i	saturation humidity in the evaporator (kg water/kg dry air)
W_{ic}	saturation humidity in the condenser (kg water/kg dry air)
z	coordinate in the flow direction (m)
x	coordinate in the flow direction (m)

Greek

α	absorptance of the collector absorber surface
λ_o	latent heat of water evaporation (J/kg)
λ_p	wall thermal conductivity (W/m/K)
λ_e	water thermal conductivity (W/m/K)
λ_c	condensed water thermal conductivity (W/m/K)
λ_G	humid air thermal conductivity in the condensation tower (W/m/K)
ρ_c	water density (kg/m^3)
μ_c	dynamic viscosity of condensed water (Ns/m^2)
τ	transmittance
η	efficiency

Subscripts

1	tower bottom
2	tower top
amb	ambient
e	cooling water at the condensation tower
w	water
o	outlet
i	inlet
g	air flowing inside the evaporation tower
G	air flowing inside the condensation tower
l	liquid

semi arid regions the lack of drinkable water often corresponds with a high solar insolation. This speaks for the use of solar energy as the driving force for water desalination systems. Especially in remote rural areas with low infrastructure and no grid connection, stand alone operating systems for the desalination of brackish or sea water are suitable to provide small settlements with clean potable water.

Solar energy has been receiving greater attention in recent years for various applications using different desalination techniques. Solar desalination systems can be divided in two main types, i.e. direct and indirect collection systems. The direct collection systems use solar energy to produce distillate directly, i.e. in the solar still, which has a single structure and does not require sophisticated technical construction or operation procedure. The solar still distillers cannot compete with the conventional methods such as multi-stage-flash (MSF), multi-effect-distillation (MED) and reverse osmosis (RO), in particular for the production of large quantities of water. However, they seem to be useful in providing small communities with fresh water with low efficiency. The low efficiency is originated from the fact that only one basin is used in which the brackish water is heated, evaporated and then condensed. Many solar stills have been constructed all over the world. To mention few of them, we cite the works of Garg and Mann [1], Rajvanshi [2], Zaki et al. [3], Delyannis [4] and Baum and Bairamov [5]. To be more competitive than the classical solar desalination system as solar still, others promising solar desalination techniques using the principle of humidification–dehumidification (HD) have been developed for the production of fresh water in remote and sunny regions [6,7].

The solar powered water desalination unit based on the HD principle can be considered as one of the performed techniques developed in solar desalination field. It is an innovative technology with promising diffusion and application due to its flexibility, simplified design, low maintenance, extended life time for over twenty years, quasi null energy consumption, low capital cost, construction and adaptation for use in rural areas to produce fresh water for drinking and irrigation [8–10].

As mentioned previously, the HD process is an interesting technique that has been widely adapted for water desalination. However, the major inconveniency of solar desalination unit especially the HD technique is their limited fresh water production. Therefore, the improvement of small solar desalination units presents an attractive solution to decentralised water demand, which is the case of remote and rural area in developing countries. There are a number of studies on the humidification–dehumidification desalination process most of which focus on performance evaluation and efficiency improvement in order to optimize the fresh water production of solar desalination units and to reduce their costs.

Veera et al. [11] studied the feasibility of round the clock operation of a low temperature desalination system powered by solar collectors with the use of thermal energy storage. Results from the theoretical study confirm that thermal energy storage is a useful component of the system for conserving thermal energy to meet the energy demand when direct solar energy resource is not available. It has been determined that a solar collector area of 18 m^2 with a thermal energy storage volume of 3 m^3 is adequate to produce 100 L/d of freshwater round the clock considering fluctuations in the weather conditions.

Karan et al. [12] used multi-parameter optimization methods to find the optimal operating conditions for both CAOW (Closed air open water) and OAOW (open air open water) humidification–dehumidification desalination cycles that result in maximum gained output ratio (GOR) and to investigate some characteristics of the various cycles. as well as open air open water cycles, each with either an air or a water heater, were considered in this analysis. Numerical optimization resulted in a substantial increase in GOR for all four cycle types compared to previous best-case conditions found using heuristic studies. The GOR of the cycles was found to decrease with increasing component terminal temperature difference (TTD). In addition, different cycles perform best at different temperature differences.

In the same year, Mehrgoo and Amidpour [13] developed a model and a structured procedure to optimize the shape and structure (relative sizes, aspect ratios) of a multi-effect humidification–dehumidification (MEH) desalination unit. The results showed that the inlet cold and hot water temperatures and the column heights play important roles in the constructal design of a MEH unit, especially as the total volume increases. Moreover, the tube diameters and the number of condenser tubes should be suitably selected based on the values of the condenser, the humidifier inlet water temperatures and the column heights.

Narayan et al. [14] and Mistry et al. [15] investigated the thermodynamic behavior of HD cycles using the First and Second Laws of Thermodynamics, respectively. Both papers discussed methods for improvement and optimization of the cycles based on thermodynamic arguments and single parameter optimization.

Zamen et al. [16] optimized the total solar HD system. Such optimization was mainly intended to reduce the fresh water production costs. They showed that solution obtained by cost objective function results in a cost 7–28% lower than other objective functions.

The present work deals with modeling, simulation and experimental validation of a new generation of water desalination unit by solar energy using a multiple effect humidification process. The main objectives of the present paper are:

- To present a steady state mathematical model of the different components of the unit (water solar collector, evaporation tower and condensation tower).
- To investigate the thermal performances of the solar desalination unit exposed to a variation of operating key parameters.
- To present numerical and experimental data as an example of the validation process that has been carried out in order to assess the credibility of the numerical models.

The present paper is organized as follows. Sections 2 and 3 are dedicated, respectively, to the process description and the developed mathematical models. Section 4 presents the computa tion process. The instrumentation and the simulation results are presented, respectively in Sections 5 and 6.

2. Process description

Figs. 1 and 2 show, respectively, a schematic diagram and a photo of the experimental setup of the humidification and dehumidification

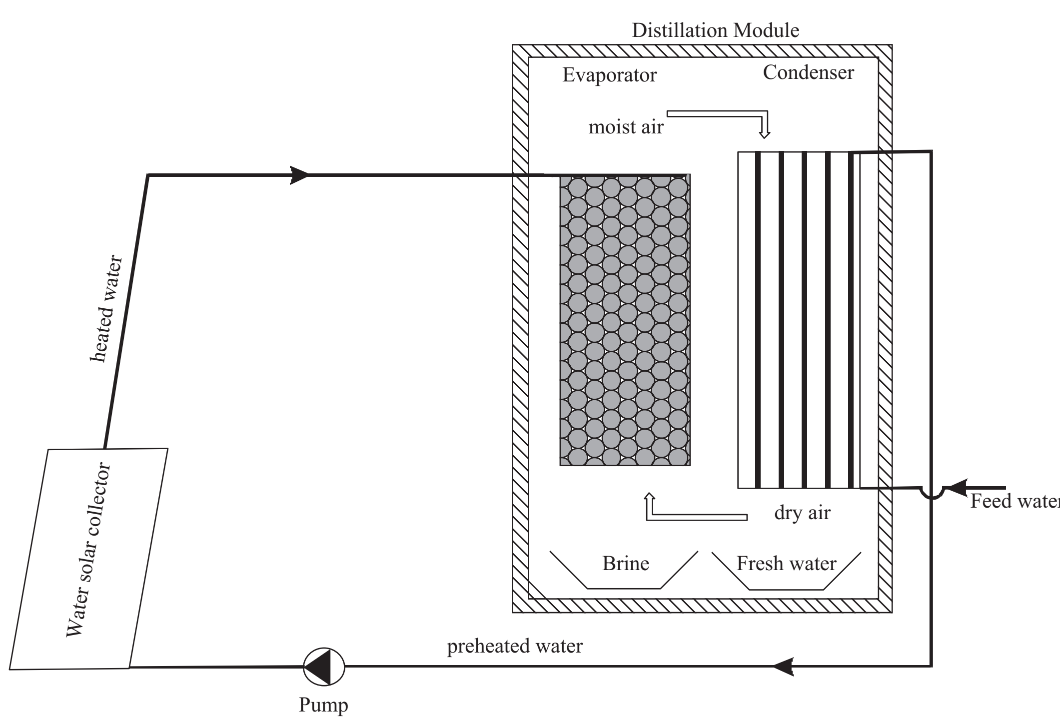


Fig. 1. Schematic diagram of the HD water desalination unit.

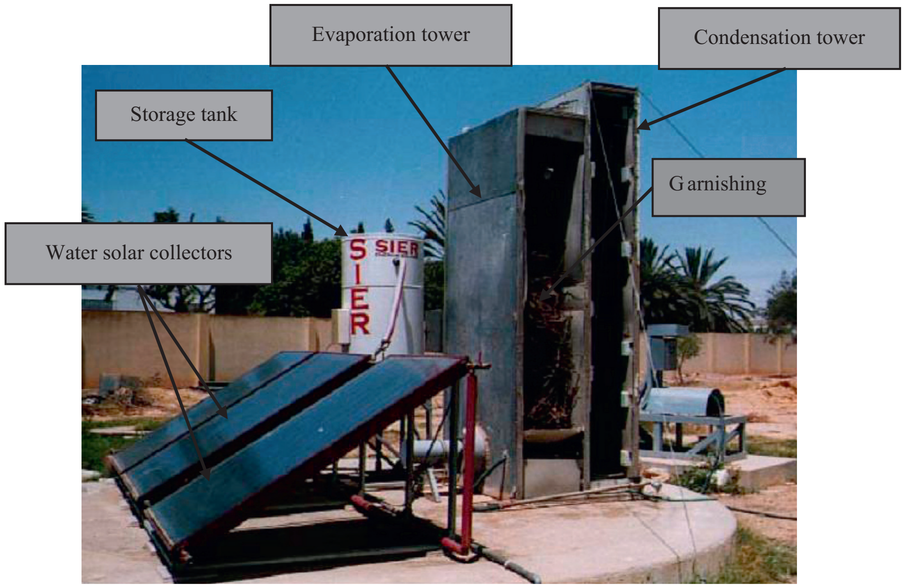


Fig. 2. A photo of the solar desalination unit experimental setup.

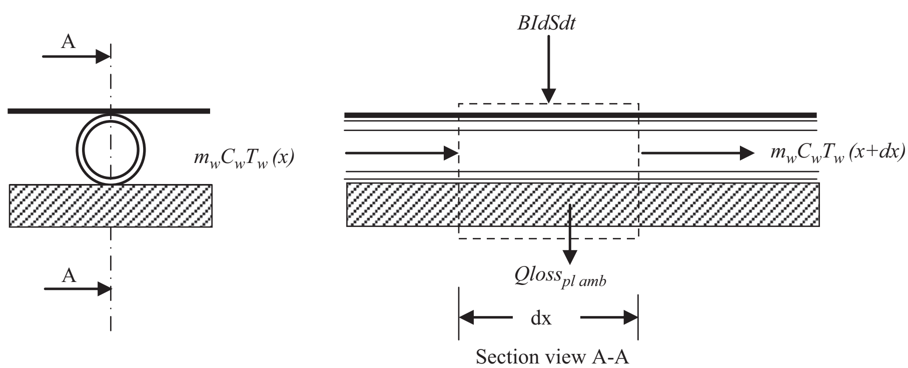


Fig. 3. Thermal energy balance of differential section of solar water collector.

(HD) water desalination unit. The developed unit operates at atmospheric pressure using air as a carrier for vapour. Three compartments constitute the installation: solar collectors, evaporation tower and condensation tower.

The principle of functioning of this desalination process is as follows. First, brackish water or sea water is heated by the solar collectors as much as possible. Then, the hot water is injected to the top of the evaporation tower. A pulverizer with a special shape is used to assure a uniform pulverisation of the hot water in all the sections of the tower. Hot and saturated air mixes with the rising air current toward the condensation tower. Then it condenses in contact with the cold condensation plates. The circulation of the air in the evaporation tower may occur in natural convection or in forced convection with two functioning modes: closed air circuit or open air circuit. In the course of working in free convection, the displacement of humid air in the ascending direction of the tower is caused by the difference of the density and temperature of the humid air in the tower. The forced convection is insured by a helical fan fixed at the bottom or at the top of the tower. The choice of the air circulation mode in the tower depends on the shape and the dimension of the packed bed.

The detailed descriptions of the unit main components are as follows:

The solar collector is the major component of the unit. In fact, its characteristics have an important influence on the operation and efficiency of the unit. It has an absorber plate containing uniformly spaced parallel copper pipes with its upper surface painted matt black to increase the absorptivity of the system. The absorber can be also made from a polypropylene material with very thin and tightly spaced capillary tubes. The fluid circulates in a forced convection and in one direction in the absorber, which is covered with a single glass of high transmissivity to solar radiation. All the parts are fitted inside an external case. The undersides of the absorber and the side casing are well insulated to reduce the heat losses to ambient air.

The evaporation tower produces the water vapour. It is equipped with packed bed to increase the contact surface and therefore improve the humidification rate. Due to the nature of the water (hot salinity level, chalky, solid residuals and corrosion problems, etc.), the packed bed used in the unit must be carefully chosen. Thorn trees or palm tree leaves are well suited for this application. They are abundant, free and have a high resistance against the forth-mentioned problems.

The condensation chamber contains polypropylene condensation plates through which the cold salty water circulates for preheating. The structure of the evaporation tower and the condensation tower is made of aluminium. The thermal insulation is achieved by Styrofoam layers with a thickness of 40 to 50 mm. To insure isolation against vapour and water circulating in the unit and to protect the Styrofoam plates against corrosion caused by brackish water, the inside of the unit is covered with polypropylene plates. The distilled water is collected in a basin at the bottom of the condensation tower. Water not evaporated is collected in a basin at the bottom of the evaporation tower and then recycled or

discarded in the case that the salt rate is too high. The two basins are made of polypropylene material. Pumps are installed to facilitate water circulation in the different parts of the desalination unit. Polypropylene ducts are used due to their resistance to corrosion.

3. Process modeling

Mathematical modeling is at the very core of the design and optimization process for thermal systems because the mathematical model brings out the important variables and the governing parameters. We have developed a mathematical model in steady state regime based on heat and mass transfers in each component of the unit i.e. water solar collector, evaporation tower and condensation tower of the desalination unit in order to numerically simulate the HD system. The developed models allow a good description of the real process and a better monitoring of the spatial distribution of the different parameters like air and water temperatures and air humidity.

3.1. Water solar collector mathematical model

Since there are no mass or concentration changes, the water solar collector can be modeled solely from thermal energy balances. To establish the model for the system, the following assumptions are considered:

- The speed of the fluid is uniform, therefore the local state of the fluid and of the absorber depends only on one side x that varies from 0 to l.
- The absorber and fluid have the same temperature at any point.
- The fluid temperature remains under the 100 °C point.

The thermal energy balance equations for the system formed by the absorber and water for a slice of the collector with a width of l, a length of dx and a surface of ds as shown in Fig. 3, is the next one:

[(The quantity of energy received by a surface absorber element, ds]=[(the quantity of energy gained by water)+(the overall losses toward the outside)]

$$I\tau\alpha\, ds = Qw + Qloss_{ab-amb} \tag{1}$$

with

$$Qw = m_w C_w dT_w$$

$$Qloss_{ab-amb} = U_w(T_w - T_{amb})\, ds$$

Eq.(1) can be written as:

$$I\,\tau\,\alpha\, ds = \quad m_w C_w dT_w \quad + \quad U_w(T_w - T_{amb})ds \tag{1'}$$

It can be also further simplified as:

$$\frac{dT_w}{dx} = \frac{U_w l}{m_w C_w}\left(\frac{\tau\alpha I}{U_w} + T_{amb} - T_w\right) \tag{1''}$$

The mathematical model for the solar collector, allows the study for constant insolation level and constant ambient temperature, the fluid temperature variation at the outlet of the collector as a function of the control, geometrical, and physical parameters (flow rate, collector area, material, and inclination angle of the collector). In addition, the fluid temperature and flow rate at the collector outlet are the two parameters with the most significant impact on the unit production as they are among the input parameters of the evaporation tower.

3.2. Evaporation tower mathematical model

The model of the evaporation tower is a set of equations developed using thermal and mass balances for the water phase, the air phase, and the air–water interface on an element of volume of height dz (Fig. 4). The approach is similar to that used in the cooling tower study [17,18].

To establish the model for the system, the following assumptions are made:

- The tower is adiabatic.
- Head losses in the tower column are low and it can be assumed that the density of the air mass flux is constant.
- Since the evaporation rate is small compared to the water flow rate, then the water mass flux remains constant throughout the column.
- The water distribution over the packed bed is uniform.

- For the water phase

The water thermal balance in an element of volume of the evaporation tower of height dz, is given by the following equation:

[The quantity of heat carried by water]=[the quantity of heat transmitted toward the surface of separation water–air]

Mathematically this can be expressed as:

$$LC_l dT_l = h_l a(T_l - T_i)dz \tag{2}$$

It can be further simplified as:

$$\frac{dT_l}{dz} = \frac{h_l a(T_l - T_i)}{LC_l} \tag{2}$$

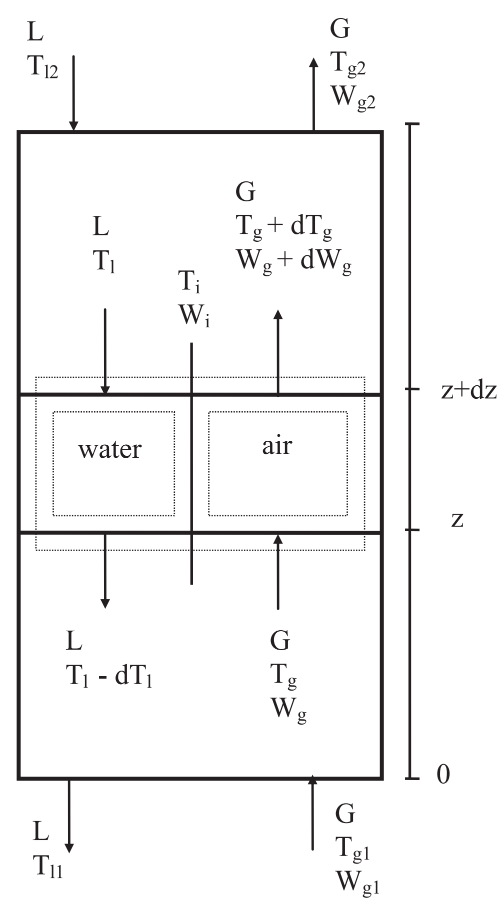


Fig. 4. An element of volume of the evaporation chamber of height dz.

- For the air phase

  The air thermal balance in an element of volume of the evaporation tower of height dz, is the following one:

  [The quantity of heat received by the surface of separation water–air]=[the quantity of heat transmitted toward the air flow rate]

  Mathematically this can be expressed as:

$$h_g a(T_i - T_g)dz = GC_g dT_g \quad (3)$$

It can be further simplified as:

$$\frac{dT_g}{dz} = \frac{h_g a(T_i - T_g)}{G\,C_g} \quad (3')$$

- Air–water interface

  At the air–water interface, the thermal balance can be written under the following shape:

  [The quantity of heat transmitted from the water current through the liquid film toward the surface of separation water–air]=[(the quantity of heat transmitted from the surface of separation through the air film toward the air current)+(the heat quantity provided to evaporate the water mass quantity transferred of the liquid, through the interface toward the air current)]

  Mathematically this can be expressed as:

$$h_l a(T_l - T_i) = h_g a(T_i - T_g) + \lambda_o k_g a(W_i - W_g) \quad (4)$$

It can be further simplified as:

$$W_i = W_g + \frac{h_l a(T_l - T_i) + h_g a(T_g - T_i)}{\lambda_o k_g a} \quad (4')$$

Also, it can be expressed as [19]:

$$W_i = 0.62198\,\frac{P_{ws}}{1 - P_{ws}} \quad (5)$$

where P_{ws} is the saturation pressure of the water vapor corresponding to a certain temperature is computed from [20] as:

$$\ln(P_{ws}) = -6096.938\frac{1}{T_i} + 21.240964 - 2.7111910^{-2}T_i + 1.6739510^{-5}T_i^2 + 2.43350\ln(T_i) \quad (6)$$

At the air–water interface, the mass balance is given by the following equation:

[The mass water quantity transferred from the interface through the air film toward air flow rate]=[the quantity of steam transmitted to air flow rate]

Mathematically this can be expressed as:

$$k_g a(W_i - W_g)dz = GdW_g \quad (7)$$

It can be further simplified as:

$$\frac{dW_g}{dz} = \frac{k_g a(W_i - W_g)}{G} \quad (7')$$

The steady state model of the evaporation tower using the equations presented above could be used to monitor the influence of the command parameters on the tower operation. In particular, it allows to determine the temperature and the amount of water in the air at the outlet of the evaporation tower as a function of the water temperature at the entrance (top of the tower) for a given tower height. The obtained model can be used to size this type of evaporation tower for desired water and air temperatures.

Due to the nature of water (hard salinity, deposits of lime stones, solid residues, corrosion problems, etc.), the garnishing to be used in this application must be chosen carefully. For instance, the thorn trees, abundant and free are appropriate under these operating conditions and their characteristics need to be specified beforehand. To do so, a set of experiments were carried out on a test bench for a cooling tower to determine the different specific heat and mass exchange coefficients at the contact surface between the garnishing and the humid air [9]. The relationships giving the mass exchange coefficients (k_g) and the heat exchange coefficients h_l as a function of the air flow rate (G) and water flow rate (L) are

$$k_g = \frac{2.09\,G^{0.11515}L^{0.45}}{a} \quad (8)$$

$$h_l = \frac{5900\,G^{0.5894}L^{0.169}}{a} \quad (9)$$

The air-film heat transfer coefficient and the mass transfer coefficient on the air–water interface are coupled by the Lewis relation [21] as follows:

$$h_g = C_g k_g \quad (10)$$

3.3. Condensation tower mathematical model

The formulation of the mathematical model of the condensation tower in the steady state regime is based on thermal and mass balances. It allows developing the coupling equations between the temperature of the cooling water of the condenser and the humid air temperature and water content. The condensation rate is determined using an algebraic equation that relates the variation of the water content with the height of the tower. The balances are done on an element of volume of the tower of height *dz* (Fig. 5).

To establish the model for the system, the following assumptions are made:

- The tower is adiabatic.
- Each stage is completely homogeneous as to avoid thermal gradients in the direction normal to the condenser plates.
- The length *dz* of the tube element is small; therefore, the temperature in each stage changes linearly throughout the length of the element.
- Colburn and Hougen method developed by Votta, which states that the sensitive heat transfer of the condensed water droplets is negligible, is used [22].
- The air heat and mass transfer coefficients at the air–water interface are related by the Lewis equation.
- The condensate film flow is normally streamlined.
- The heat flows through the film by conduction.

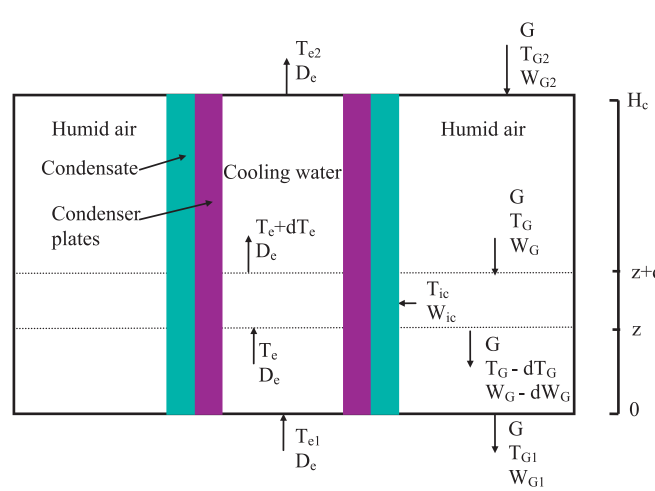


Fig. 5. An element of volume of the condensation chamber of height *dz*.

The mathematical model for the condensation tower is formed by the following system of equations:

- For the water phase
  [The quantity of heat transmitted from air–water interface to water in the condenser]=[the quantity of heat carried away by water]
  Mathematically this can be expressed as:

$$UA(T_{ic}-T_e)dz = D_eC_edT_e \tag{11}$$

It can be further simplified as:

$$\frac{dT_e}{dz} = \frac{UA(T_{ic}-T_e)}{D_eC_e} \tag{11′}$$

- For the air phase
  [The quantity of heat carried by air]=[(sensible heat quantity transmitted toward the surface of separation air–water)–(latent heat quantity due to the condensation of steam transmitted to the surface of separation air–water)]
  Mathematically this can be expressed as:

$$GC_GdT_G = h_GA(T_G-T_{ic})dz - \lambda_o k_GA(W_{gc}-W_{ic})dz \tag{12}$$

It can be further simplified as:

$$\frac{dT_G}{dz} = A\frac{(h_G(T_G-T_{ic}) + \lambda_o k_G(W_G-W_{ic}))}{GC_G} \tag{12′}$$

- At the air–condensate interface
  The heat balance at air–condensate interface is given by the following equation:
  [(cooling sensible heat quantity of humid air received by air–condensate interface)+(latent heat quantity liberated during the condensation at air–condensate interface)]=[quantity of heat transmitted from air–condensate interface to the cooling water]
  Mathematically this can be expressed as:

$$h_GA(T_G-T_{ic})dz + \lambda_o k_GA(W_G-W_{ic})dz = UA(T_{ic}-T_e)dz \tag{13}$$

It can be further simplified as:

$$W_{ic} = W_G + \frac{h_G(T_G-T_{ic}) + U(T_e-T_{ic})}{\lambda_o k_G} \tag{13′}$$

also, it can be expressed as [19]:

$$W_{ic} = 0.62198\frac{P_i}{1-P_i} \tag{14}$$

where P_i is the saturation pressure.

The mass balance at air–condensate interface is given by the following equation:

[The quantity of air transferred toward air–water interface]=[the quantity of steam condensed]

Mathematically this can be expressed as:

$$K_GA(W_{gc}-W_{ic})dz = GdW_G \tag{15}$$

It can be further simplified as:

$$\frac{dW_G}{dz} = k_GA\frac{(W_G-W_{ic})}{G} \tag{15′}$$

Following the water balance equation:

$$dm_c = GdW_G \tag{16}$$

So the flow rate of the condensed water is:

$$dm_c = k_GA(W_{ic}-W_G)dz \tag{17}$$

For a flow between two vertical plates, the heat transfer coefficient h_G is given by [17]:

$$h_G = \frac{\lambda_G}{D_{h1}}0.779(Gr^{1/4}) \tag{18}$$

The coefficient k_G is determined using the Lewis relation:

$$k_G = \frac{h_G}{C_G} \tag{19}$$

The overall heat transfer coefficient from the air–condensate interface to the cooling water inside the condenser is approximated by [9]:

$$U = \frac{1}{\left(\frac{1}{h_c}\right) + \left(\frac{e}{\lambda_p}\right) + \left(\frac{1}{h_e}\right)} \tag{20}$$

where h_e is given by [23]:

$$h_e = 0.023\frac{\lambda_e}{D_{h2}}Re^{0.8}Pr^{0.33} \tag{21}$$

and h_c is expressed using the Nusselt relation [23]:

$$h_c = \sqrt[4]{\frac{\rho_c^2 g\lambda_o\lambda_c^3}{4\mu_c z(T_{ic}-T_p)}} \tag{22}$$

The steady state model developed allows finding the influence of the command parameters on the tower operation and the sizing of this type of condensation tower for desired amount of distilled water m_c produced by the unit.

4. Computational process

The model equations developed in the preceding section are composed of a set of highly interlinked nonlinear equations. Therefore, iterative solution is necessary to calculate the system characteristics for each unit components. Moreover, since these components are coupled and the output of each component is the input of the next, it is necessary to couple the various components of the present desalination unit and get a global steady state mathematical model that would provide a good description of the entire system. Fig. 6 gives a general picture of the flow chart of the computer model.

A computation program was compiled in terms of the system model to predict the system performance. The calculation procedure of the program is as follows:

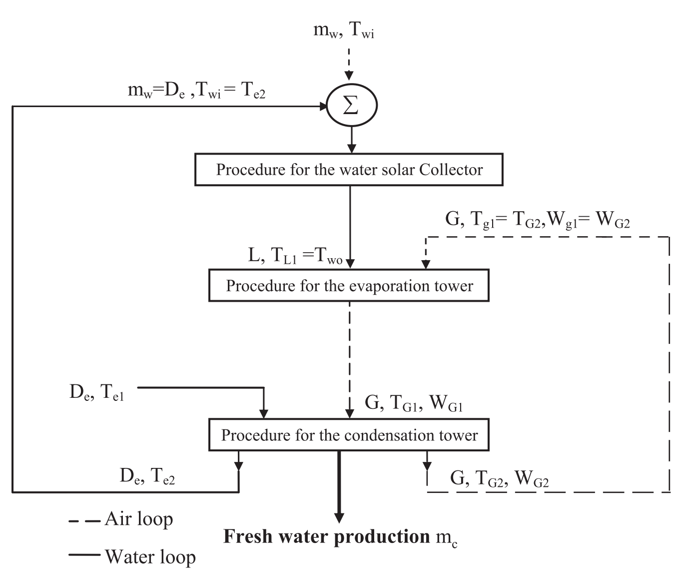


Fig. 6. A general picture of the flow chart of the computer model.

1. Input the known data for each unit components, such as the functioning parameters and the geometric parameters.
2. Calculate the data concerning the water solar collector and obtain the temperature of feed water to the evaporator.
3. Calculate the data concerning the evaporation tower and obtain evaporation rate, outlet temperature of seawater, outlet temperature and humidity of the air.
4. Calculate the data concerning condenser to obtain the outlet temperature and humidity of the air, outlet temperature of the cooling water and the fresh water production in particular.
5. Calculate the indexes of system performance and output the results.

5. Instrumentation

The measured variables in the experiment include inlet and outlet air and water temperatures in each unit components, ambient temperature, air velocity and the solar irradiation incident on the field collector's plane. The water solar collector was instrumented with Pt 100 thermistors for measuring the outlet and the inlet of water temperatures and ambient temperature. The Pt 100, which measured the ambient temperature, was kept in a shelter to protect the sensor from direct sunlight. The inlet and the outlet water and air temperatures in both the evaporation tower and the condensation tower were measured using the TH 100 transmitter. The water inlet flow rate was measured using a flow meter, while the fresh water flow rate was measured by graduated cylinder. A pyranometer was used to measure the total solar irradiation placed in a horizontal plane adjacent to the collector. All sensors, which were calibrated before using to determine the probes sensibility, were connected to a data acquisition system (type Agilent 34970 A). The detailed technical specifications of sensors and probes used in experimental set up are presented in Table 1.

6. Results and discussion

Simulation is the process of subjecting the model for a given thermal system to various inputs, such as operating conditions, to determine how it behaves and thus predict the characteristics of the actual physical system. Though simulation may be carried out with scale models and prototypes, the expense and effort involved generally makes it impossible to use these for design because many different designs and operating conditions need to be considered and evaluated.The characteristics of the pilot desalination unit used in simulation are listed in Table 2.

6.1. Thermal performance

The solar desalination unit was designed originally to reduce the thermal energy consumption necessary for heating water in the solar collector by internally recovering the latent heat of vaporisation. For this purpose, the feed water was preheated in the condenser by exchange of heat with the vapour at condensation. The coolant water passes the condenser plates in counter flow to the hot feed water and is gradually warmed by the latent heat of condensation. When the coolant water comes out of the condenser it is fed to the flat plate solar collector for further heating. In thermal desalination processes the gained output ratio (GOR) and the thermal efficiency of the solar collector are the two most commonly encountered parameters for the evaluation and assessment of such systems. The GOR can either be defined as a mass ratio (kg distillate produced/kg steam consumed) or as an energy ratio. The drawback of the mass ratio definition is that it ignores the amount of heat transferred from the steam to the product water and reject brine. As an energy ratio the GOR is defined as the total latent heat of evaporation of the product water to the input thermal energy. Theoretical energy required to produce the distillate divided by the actual thermal energy consumed in the evaporator. Mathematically, the GOR of the solar desalination unit can be written as [24,25]:

$$GOR = \frac{m_c \lambda_o}{LC_l(T_{l2} - T_{l1})} \tag{23}$$

where m_c is the condensation flow rate, L is the water mass flow rate in the evaporation tower, and λ_o is the latent heat of vaporization.

The thermal efficiency of the water solar collector was evaluated by comparing the total radiant heat energy flux to the energy gained water after passage through the collector. This is given in the following equation [24]:

$$\eta = \frac{m_w C_w (T_{wo} - T_{wi})}{I\,S} \tag{24}$$

where m_w is the water mass flow rate, C_w is the water heat capacity, T_{wo} is the water outlet temperature, T_{wi} is the water inlet

Table 2
Characteristics of the pilot desalination unit.

Solar collector	
Area	7.20 m^2
Effective transmission absorption	0.83
Riser tube material	Copper
Absorber surface	Pain mat black
Loss coefficient	3.73 $W/m^2/K$
Back insulation, thickness, mm	Fibre glass, 50
Evaporation chamber	
Size	1.20 m × 0.50 m × 2.55 m
Packed bed type	Solid packing: thorn trees
Mass transfer coefficient	$k_g = (2.09 \times G^{0.11515} \times L^{0.45})/a$
Heat transfer coefficient	$h_l = (5900 \times G^{0.5894} \times L^{0.169})/a h_g = C_g \times k_g$
Condensation tower	
Size	1.2 m × 0.36 m × 3.0 m
Plates type	Polypropylene

Table 1
Sensors and probes used in experimental set up.

Sensor/type	Reference	Description	Value
Pt 100	PRO-SL 100 PV	Sensibility	0.3799 Ω/°C
TH 100	KIMO TH 100-AOD	Humidity	
		Accuracy	±2%
		Sensibility	0.159 mA/%
		Temperature	
		Accuracy	±0.2 °C
		Sensibility	0.160 mA/°C
Pyranometer CE 180	CIMEL CE 180	Accuracy	1%
		Sensibility	12.29 μV/Wm^2

temperature, I is the solar irradiation intensity and S is the collector area.

Figs. 7 and 8 show the thermal efficiency variation of water solar collector as a function, respectively, of water mass flow rate and inlet water temperature for different values of solar radiation. Fig. 7 presents that the thermal efficiency of the water solar collector increases with the increase of the water flow rate. This may be due to the fact that for high flow rates, the collector operating temperature would be lower, resulting in lower heat losses and, subsequently, higher efficiency. In addition, for water flow rate values higher than 0.4 kg/s one notes that an asymptotic regime was reached during which the increase in the water flow rate is useless. Fig. 8 shows that the thermal efficiency of the water solar collector decreases with an increase of the inlet water temperature (T_{wi}). On one hand, for inlet water temperature values inferior to ambient temperature, the thermal efficiency increases with a decrease of solar radiation intensity. On the other hand, for inlet water temperature values superior to ambient temperature, the thermal efficiency decreases with a decrease of solar radiation intensity. From Fig. 8, one can also notes that for an inlet water temperature equal to the ambient temperature, the solar radiation intensity has no effect on the thermal efficiency of the water solar collector.

The variation of the gain output ratio with cooling water mass flow rate at the condensation tower and water mass flow rate at the evaporation tower are presented, respectively in Figs. 9 and 10. A slight decrease of the GOR is observed in Fig. 9. When cooling water mass flow rate is increased and then stabilizes. Fig. 10 illustrates that the optimal water mass flow rate is about 0.4 kg/s, of which the GOR is maximum. The GOR of the system is 3. This result can be explained by the fact that while increasing the water mass flow rate inside the evaporation tower, the rate of vaporisation increases which in its part augments the fresh water production, hence, the GOR.

6.2. Experimental validation

The validation of the model developed for a given system is another very important consideration because it determines whether the model is a faithful representation of the actual physical system and indicates the level of accuracy that may be expected in the predictions obtained from the model. To validate the developed models of the desalination unit, a series of experiments was conducted using the pilot desalination unit located at the National Engineering School of Sfax (E.N.I.S)—Sfax University, Tunisia. Experimental measurements were taken on the solar collector and the distillation module (evaporation and condensation chambers).

Fig. 11 illustrates a comparison between predicted and measured collector outlet temperature (T_{wo}) as a function of solar radiation. It is apparent, as expected, that for a constant water flow

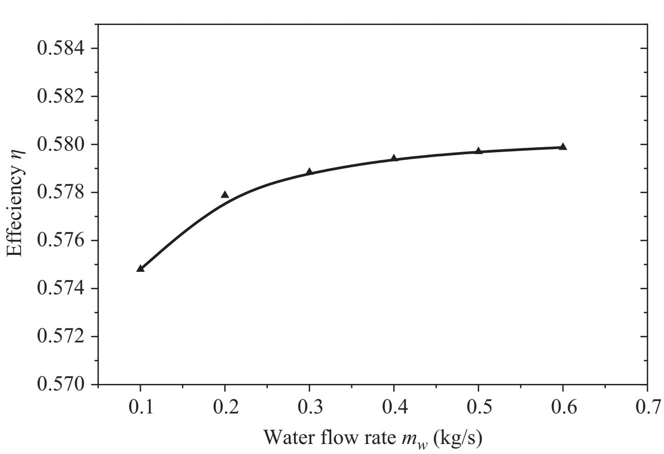


Fig. 7. Effect of the water mass flow rate on the collector thermal efficiency. (T_{wi}=20 °C, T_{amb}=30 °C).

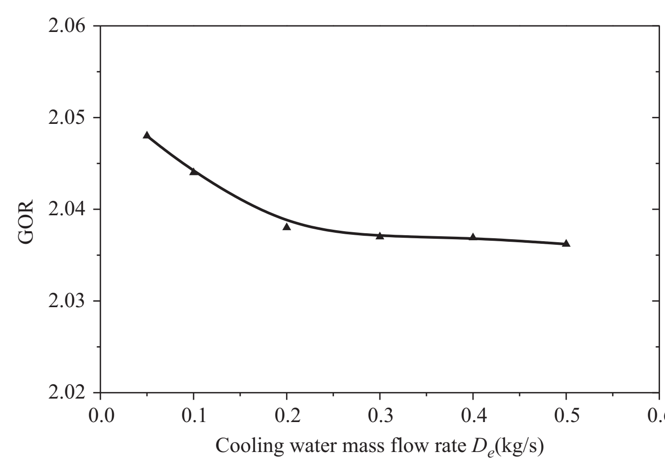


Fig. 9. Effect of the cooling water mass flow rate at the condensation tower on GOR (T_{e1}=20 °C, L=0.2 kg/s, G=0.1 kg/s).

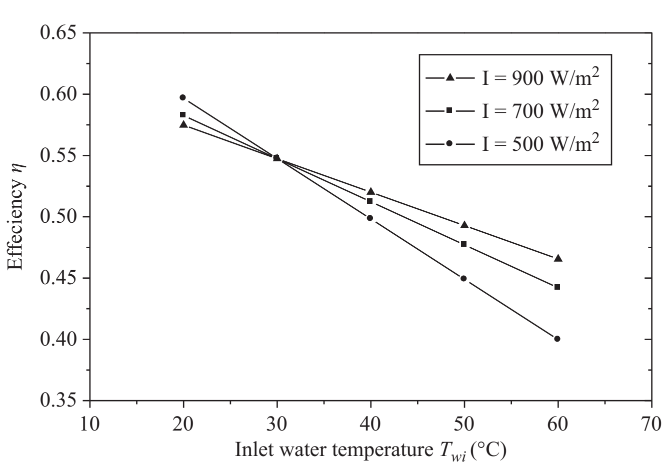


Fig. 8. Effect of the inlet water temperature on the collector thermal effeciency for different values of solar radiation (m_w=0.1 kg/s, T_{amb}=30 °C).

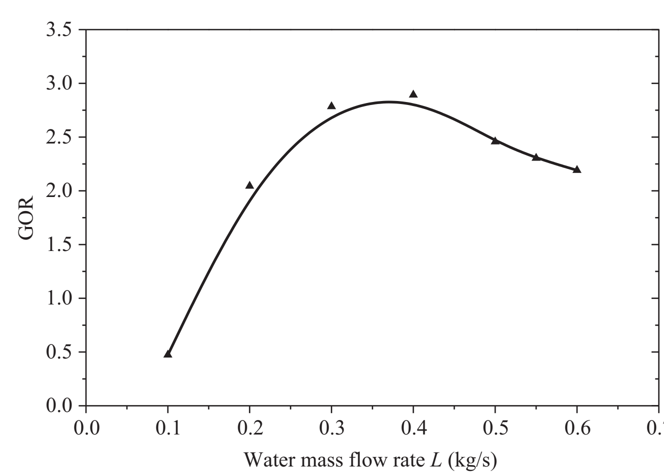


Fig. 10. Effect of the water mass flow rate at the evaporation tower on GOR (T_{e1}=20 °C, D_e=0.1 kg/s, G=0.1 kg/s).

rate the outlet water temperature increases with solar radiation. It can be also seen that a good agreement had been found between the simulated and the experimental results.

Fig. 12 shows a comparison between the experimental and the theoretical values of air absolute humidity (W_{g2}) as a function of inlet water temperature at the level of the evaporation tower. It is clear from this figure that the amount of water in the humid air at the top of the evaporation tower increases significantly as the water temperature (T_{l2}) at the evaporation tower inlet increases. It can be also noticed that the theoretical curve of water content W_{g2} as a function of the temperature T_{l2} exceeds the experimental curve, as seen in Fig. 12. The gap between the theoretical and experimental values increases with T_{l2}. This may be due to the thermal losses that increase with the temperature, even though the process is assumed to be theoretically adiabatic.

Fig. 13 shows a comparison between the measured and the calculated cooling water temperature at the exit of the condensation tower as a function of inlet water temperature at the entrance of the evaporation tower. Through this figure one can note that increasing the evaporation tower inlet water tempertaure leads to a significant increase in the condensation tower outlet cooling water temperature. This may be due to the fact that an increase of the inlet water temperature in the evporator increases the outlet moist air temperature leaving the latter to the condenser. Consequently, the outlet cooling water temperature increases due to the latent heat of condensation. It was also noticed that the experimental values were less than the theoretical ones. This may be attributed partly to the fact that the theoretical model assumes that each stage is completely homogeneous as to avoid thermal gradients in the direction normal to the condenser plates.

Figs. 14 and 15 show a comparison between the experimental and the theoretical values of the outlet fresh water flow rate (m_c) as a function, respectively, of the water temperature at the evaporator inlet and the air temperature at the condenser inlet. From this figure we can note that the flow rate of the fresh water increases with increasing air and water temperatures. This may be explained by the fact that increasing the air and water temperatures at the entrance of the evaporation tower and the condensation one produces more thermal energy inside the solar desalination unit which in its part increases the quantity of evaporated water. This leads to increasing the fresh water flow rate.

For a given water temperature at the entrance of the evaporation tower (T_{l2}), and knowing the experimental values of m_c, W_{G1} and W_{G2}, the humid air mass velocity is [9]:

$$G_{\text{exp}} = \frac{m_c}{(W_{G2} - W_{G1})} \tag{25}$$

Using this equation, the air circulates in the unit with a speed lower than the theoretical one. Tests show that $G_{\text{exp}} \cong 0.60 \times G_{\text{th}}$. The decrease in the air flow rate is compensated by an increase in

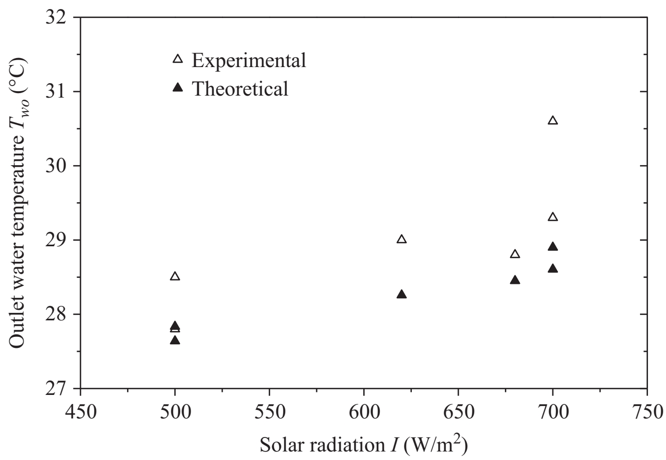


Fig. 11. Impact of solar radiation on the solar collector outlet temperature.

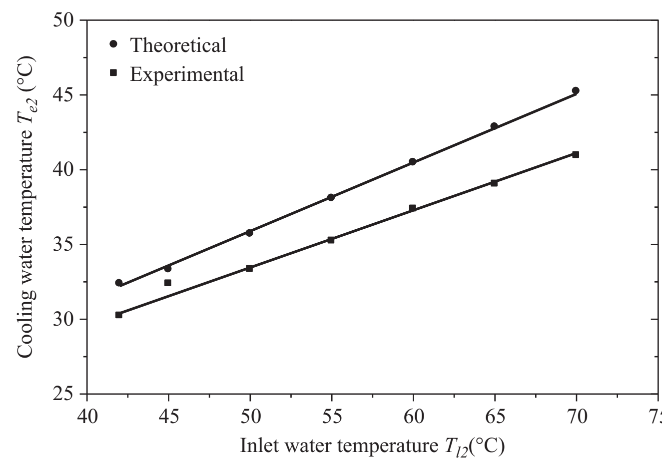


Fig. 13. Cooling water temperature variation at the condensation tower exit as a function of water temperature at the evaporation tower inlet.

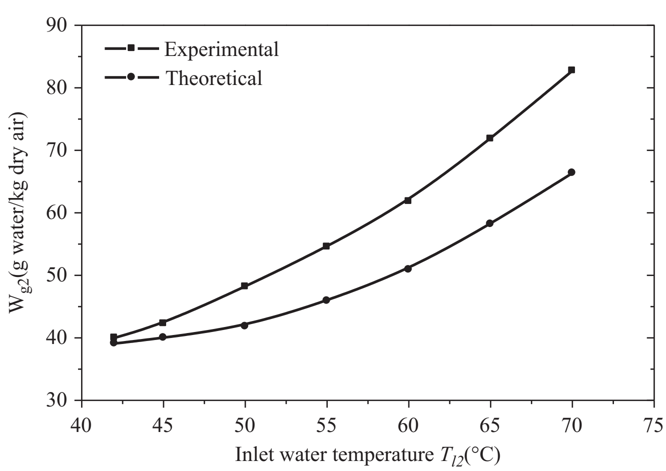


Fig. 12. Air humidity variation at the top of the evaporation tower as a function of water temperature at the evaporation tower inlet.

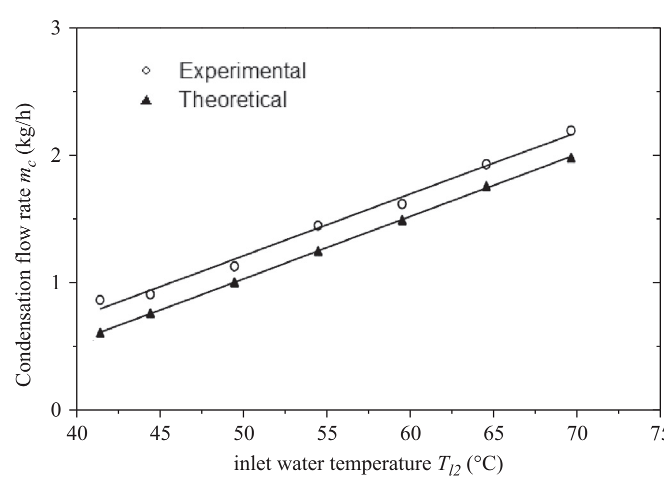


Fig. 14. Variation of the condensation flow rate as a function of water temperature at the evaporation tower inlet.

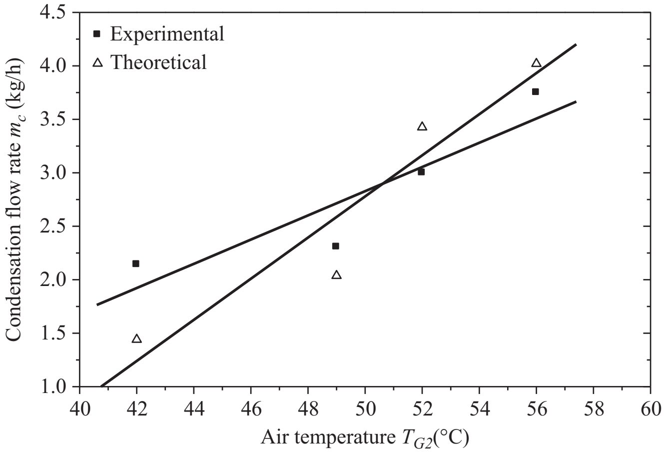


Fig. 15. Variation of the condensation flow rate as a function of air temperature at the condensation tower inlet.

Table 3
The accuracy of the experimental results.

Parameter	Average relative error ε_{ar} (%)	Maximum absolute error ε_{max} (°C)	Minimum absolute error ε_{min} (°C)
T_{wo}	2.468	1.99	3.5×10^{-2}
W_{g2}	13.304	16.36	9.1×10^{-1}
T_{e2}	7.683	4.28	9.5×10^{-1}
m_c (as a function of T_{l2})	7.786	5.31	6.3×10^{-1}
m_c (as a function of T_{G2})	4.347	1.5	4.7×10^{-2}

With:$\varepsilon_{max}=\max|T_{exp}(i)-T_{sim}(i)|$, $\varepsilon_{min}=\min|T_{exp}(i)-T_{sim}(i)|$, $i=1, 2,\ldots,k$.

the difference between the air temperatures at the top and that at the bottom of the condensation tower. This is why the actual water distillation rate is close to or sometimes higher than the theoretical rate, as seen in Figs. 14 and 15.

6.3. Experimental error

Table 3 presents a simple statistical analysis of the relative error between simulation and experimental measurements. The accuracy of the experimental results may be calculated using the following definition [26]:

$$\varepsilon_{ar}(\%)=\frac{100}{k}\sum_{i=1}^{k}\frac{|T_{exp}(i)-T_{sim}(i)|}{T_{exp}(i)} \tag{26}$$

where T_{exp} denotes the experimental data of T, while, T_{sim} and k are the theoretical prediction of T and the number of experimental measurements, respectively. The error analysis of the different validated parameters shown in Figs. 11–15 is presented in Table 3. It is clear from this table that the agreement between experiment data and the results calculated from the theoretical prediction of the present device is fairly good. The maximum average relative error was found to be about 13% for the absolute air humidty. This value was expected due to uncertainties in the measured quantities of the experiments and the simplifying assumptions in the mathematical models in addition to the computational errors and the accuracy of calculations.

7. Conclusion

Brackish water or seawater desalination can be an interesting alternative to guarantee a secure source of water. Solar energy is considered as one of the most sustainable way to supply the energy needs for desalination, since it can be offered close to the desalination plants where connection to the public electric grid is either not cost effective or not feasible and avoid environmental problems associated with fossil fuels. Therefore, the improvement of small desalination units presents an attractive solution to decentralised water demand, which is the case of remote and rural area in developing countries. The presented unit can be considered as one of the best choice for production of fresh water due to its flexibility, simplified design, low maintenance, extended life time for over twenty years, quasi null energy consumption, construction and adaptation for use in rural areas.

In this paper, a steady state mathematical model expressing the heat and mass transfers in each component of the unit is formulated. The developed model is simulated to study the influence of operating conditions on the thermal performance of the unit. It was found that:

- The GOR increases with increasing the water mass flow rate at the inlet of the evaporation tower. There is an optimum value of the water mass flow rate where the GOR is maximum. The optimal water mass flow rate is about 0.4 kg/s.
- The GOR decreases with increasing water mass flow rate inside the condensation tower and then stabilizes.
- The thermal efficiency of the water solar collector increases with the increase of the water mass flow rate.
- The thermal efficiency of the water solar collector decreases with an increase of the inlet water temperature.
- The thermal efficiency decreases with a decrease of solar radiation intensity.
- For an inlet water temperature equal to the ambient temperature, the solar radiation intensity has no effect on the thermal efficiency of the water solar collector.

Experimental results were compared with the simulation results. It was shown that the developed models are able to predict accurately the trends of the heat and mass characteristics of the evaporation and condensation chambers and the solar collectors. As a result, the proposed models can be used for sizing and testing the behaviour of such a type of desalination unit.

References

[1] Garg HP, Mann HS. Effect of climatic, operational and design parameters on the year round performance of single-sloped and double-sloped solar still under Indian arid zone conditions. Solar Energy 1976;18:63–159.
[2] Rajvanshi AK. Effect of various dyes on solar distillation. Solar Energy 1981;27:51–65.
[3] Zaki GM, Radhwan AM, Balbeid AO. Analysis of assisted coupled solar still. Solar Energy 2003;75:93–381.
[4] Delyannis A. The Patmos solar distillation plant. Solar Energy 1968;11:113–5.
[5] Baum VA, Bairamov R. Prospects of solar stills in Turkmenia. Solar Energy 1966;10:38–40.
[6] Rodriguez LG. Renewable energy applications in desalination: state of the art. Solar Energy 2003;75:93–381.
[7] Parekh S, Farid MM, Selman JR, Al Hallaj SA. Solar desalination with humidification–dehumidification technique—a comprehensive technical review. Desalination 2004;160:168.
[8] Bohner A. Solar desalination with a high efficiency multi effect process offers new facilities. Desalination 1989;73:197–203.
[9] Ben Bacha H. Modélisation et simulation en vue de la commande d'une unité de dessalement d'eau par l'énergie solaire, thèse de doctorat. Tunis University, ESSTT, Tunisia 1996.
[10] Ben Bacha H, Maalej AY, Ben Dhia H, Ulber I, Uchtmann H, Engelhardt M, Krelle J. Perspectives of solar powered desalination with SMCEC technique. Desalination 1999;122:177–83.
[11] Gude VeeraPlease check author names as first name has appeared both in abbreviated and full form, throughout the reference listGnaneswar, Nirmalakhandan Nagamany, Deng Shuguang, Maganti Anand. Low temperature desalination using solar collectors augmented by thermal energy storage. Applied Energy 2012;91:466–74.

[12] Karan H, Mistry Alexander, Mitsos, John H, Lienhard V. Optimal operating conditions and configurations for humidificationede humidification desalination. International Journal of Thermal Sciences 2011;50:779–89.
[13] Mehrgoo Morteza, Amidpour Majid. Derivation of optimal geometry of a multi-effect humidification–dehumidification desalination unit: a constructal design. Desalination 2011;281:234–42.
[14] Narayan GP, Sharqawy MH, Lienhard JH, Zubair SM. Thermodynamic analysis of humidification dehumidification desalination cycles. Desalination and Water Treatment 2010;16:339–53.
[15] Mistry KH, Lienhard JH, Zubair SM. Effect of entropy generation on the performance of humidification–dehumidification desalination cycles. Int. J. Therm. Sci. 2010;49:1837–47.
[16] Zamen M, Amidpour M, Soufari SM. Cost optimization of a solar humidification dehumidification desalination unit using mathematical programming. Desalination 2009;239:92–9.
[17] Kaguel S, Nishio M, Wakao N. Parameter estimation for packed cooling tower operation using a heat input-response technique. International Journal of Heat and Mass Transfer 1988;31:2579–85.
[18] Younis MA, Fahim MA, Wakao N. Heat input-response in cooling tower- zeroth moments of temperature variations. J. Chem. Eng. Jpn 1987;20:614–8.
[19] Wexler A. Vapor pressure formulation for water in range 0 to 100 °C. Journal of Research of the National Bureau of Stantards A: Physics and Chemistry 1976;80:775–85(A) 1976;80:775–85.
[20] ASHRAE. Fundamental Handbook TomeV 1977.
[21] Ben Bacha H, Maalej AY, Ben Dhia H. A methodology to predict operation of a solar powered desalination unit. Advanced research workshop. In: InRizzuti L, Ettouney HM, Cipollina A, editors. Solar Desalination for the 21st Century. Dordrecht, The Netherlands: Springer; 2007. p. 69–82.
[22] Grehier A, Rojey A. Echangeurs à condensation en matériau polymère. Revue de l'Institut Français du Pétrole 1989;1:77–89.
[23] Sacadura JF. Initiation aux transferts thermiques, Fourth printing. Techniques et Documentation 1993:251–60.
[24] Banat Fawzi, Jwaied Nesreen, Rommel Matthias, Koschikowski Joachim. Marcel Wieghaus. Desalination by a compact SMADES autonomous solar-powered membrane distillation unit. Desalination 2007;217:29–37.
[25] Koschikowski J, Wieghaus M, Rommel M. Solar thermal-driven desalination plants based on membrane distillation. Desalination 2003;156:295–304.
[26] Zhani K, Ben Bacha H, Damak T. Modeling and experimental validation of a humidification–dehumidification desalination unit solar part. International Journal of Energy 2011;36:3159–69.